Dalton Transactions

Accepted Manuscript

ROYAL SOCIETY OF CHEMISTRY

www.rsc.org/dalton

Journal Name

RSCPublishing

ARTICLE

A Computational Study of the Mechanism for Water Oxidation by (bpc)(bpy)$Ru^{II}OH_2$

Cite this: DOI: 10.1039/xoxxoooooox

Ying Wang and Mårten S. G. Ahlquist*

Received ooth January 2012,
Accepted ooth January 2012

DOI: 10.1039/xoxxoooooox

www.rsc.org/

A mechanistic study on the catalytic cycle water oxidation with **1** $[(bpc)(bpy)Ru^{II}OH_2]^+$ (Hbpc = 2,2'-bipyridine-6-carboxylic acid, bpy = 2,2'-bipyridine) is described in this paper. Stepwise oxidation via proton-coupled electron transfer gives **3** $[(bpc)(bpy)Ru^{IV}=O]^+$. An active **4** $[(bpc)(bpy)Ru^{V}=O]^{2+}$, which is involved in the OO bond formation is generated from further $1e^-$ oxidation of **3**. Another different possible reaction at **4** was investigated and new destructive paths involving overoxidation of the metal were identified. The most viable path for OO bond formation via a water nucleophilic attack at the oxo of **4** is found to be the rate-determining step in this water oxidation catalytic cycle, and the hydro-peroxo **6** $[(bpc)(bpy)Ru^{III}OOH]^+$ is generated accompanied with a proton transfer. The super-oxo $\mathbf{7}_{\text{side-on}}$ $[(bpc)(bpy)Ru^{IV}OO]^+$ and $\mathbf{8}_{\text{side-on}}$ $[(bpc)(bpy)Ru^{V}OO]^{2+}$, both low spin species, are generated by further oxidations of **6**. Through an intersystem crossing they can transform to their high spin states, $\mathbf{9}_{\text{end-on}}$ $[(bpc)(bpy)Ru^{IV}OO]^+$ and $\mathbf{12}_{\text{end-on}}$ $[(bpc)(bpy)Ru^{V}OO]^{2+}$, respectively. Following a dissociative pathway O_2 is readily generated from both $\mathbf{9}_{\text{end-on}}$ and $\mathbf{12}_{\text{end-on}}$.

Introduction

Water splitting driven by light[1] is currently attracting considerable attention due to its potential to solve the energy storage problem by converting solar energy to chemical energy. This process includes two vital half-cell reactions: water oxidation to produce O_2 and proton reduction to generate H_2. One of the challenges to make this process success is the development of efficient and robust catalyst for water oxidation.[2] Considerable progress has been made in constructing new water oxidation catalysts based on Ru,[3] Ir,[4] and some first-row transition metals[5] such as iron, copper, cobalt and so forth, since complex *cis,cis*-$[(bpy)_2(H_2O)Ru^{III}\text{-}O\text{-}Ru^{III}\text{-}(H_2O)(bpy)_2]^{4+}$ (bpy = bipyridine) normally referred to as the blue dimer[6] due to its deep blue color, was first reported by Meyer's group. In recent years a new family of mononuclear ruthenium complexes carrying anionic ligands were found to have good performance for water oxidation,[7] and some of them even show a comparable performance (using Ce^{4+} as a chemical oxidant) with the oxygen-evolving complex in photosystem II.[8] There is a clear advantage of having anionic ligands that can modulate the reduction potentials of the catalysts.[7e] Creating new families of related Ru complexes by changing to other anionic ligands is synthetically feasible.

Along with the development of water oxidation catalysts with better performance, more attention is on elucidating the relevant possible water oxidation mechanisms. A well-defined mechanistic study for water oxidation catalyzed by $[Ru(tpy)(bpm)(OH_2)]^{2+}$ (tpy = terpyridine; bpm = 2,2'-bipyrimidine) has been reported by the Meyer group,[9] where they proposed that the OO formation is completed by water attack on $Ru^{V}=O^{3+}$ and the rate-limiting step in the catalytic cycle is the O_2 release from $[Ru^{IV}(OO)]^{2+}$ (excess Ce^{IV}, 0.1 M HNO_3). The rate-limiting step in the cycle changes to further oxidation from $[Ru^{IV}(OO)]^{2+}$ to $[Ru^{V}(OO)]^{3+}$ followed by rapid O_2 generation when performed in a more oxidizing environment (excess Ce^{IV}, 1.0 M HNO_3). Several related studies[10] have also reported similar proposals for OO bond formation, involving water nucleophilic attack to an M=O. Another pathway involving interaction of two M-O entities for OO bond coupling has been found to operate in some cases. One study on an intramolecular OO bond formation been reported by the Llobet group.[11] OO bond formation via intermolecular coupling proposal was first reported by the Sun group, and the kinetics of catalytic water oxidation were tested to be second order in complex $Ru(bda)(pic)_2$ (H_2bda = 2,2'-bipyridine-6,6'-dicarboxylic acid; pic = 4-picoline), which indicating that the catalytic reaction proceeds thought a dimeric complex.[12a] Following this a computed binuclear pathway was completed by Privalov and coworkers in 2010.[12b] They found that the potential-energy barrier for the direct OO coupling (between two metal oxyl radicals) is low and the dissociation of

O_2 from a peroxo intermediate does not require a high-energy ligand substitution. Just in 2014 a study was published,[13] where they introduced a new oxidatively rugged dinuclear water oxidation catalyst, which is generated from its corresponding mononuclear counterparts by self-assembly. For the first time the authors found that two interconnected catalytic cycles coexist, whereby the mononuclear system can be irreversibly converted into the more stable dinuclear system via a coupling between Ru^{II}-OH_2 and Ru^{VI}=O complexes.

One new water oxidation catalyst $[(bpc)(bpy)Ru^{II}OH_2]^+$, which contains the tridentate mono-anionic bpc ligand (Hbpc = 2,2'-bipyridine-6-carboxylic acid), was prepared just recently.[14] The incorporation of this mono-anionic ligand at the ruthenium complex gives a catalyst with the ability of water oxidation along with an increased solubility in water, which allowed for detailed experimental studies of the mechanism, which in turn provides important information for detailed atomistic studies using computational tool. Herein we present a study of the full mechanism of water oxidation by $[(bpc)(bpy)Ru^{II}OH_2]^+$. We have identified the rate limiting step as well as crucial steps towards the degradation of the catalyst that should be avoided in order to achieve high turnover numbers that are necessary for a functional device.

Results and discussion

1) Oxidation steps from 1 to 4.

Ru-aqua complexes are capable of reaching high valent states by losing protons and electrons sequentially and simultaneously.[15] The specific type and order of these processes varies for different kinds of catalysts. Oxidation of **1** to **2** $[(bpc)(bpy)Ru^{III}OH_2]^{2+}$ is a one-electron transfer process at pH 0, and the reduction potential of $Ru^{III/II}$ couple is calculated to be 0.83 V. The following oxidation from **2** to **3** $[(bpc)(bpy)Ru^{IV}=O]^+$ is a two-proton coupled one electron transfer process with a calculated potential of 1.52 V. The highly electrophilic **4** $[(bpc)(bpy)Ru^{V}=O]^{2+}$ is generated after a subsequent oxidation of **3** (Scheme 1). The redox potential of $Ru^{V/IV}$ is calculated to be at 1.77 V.

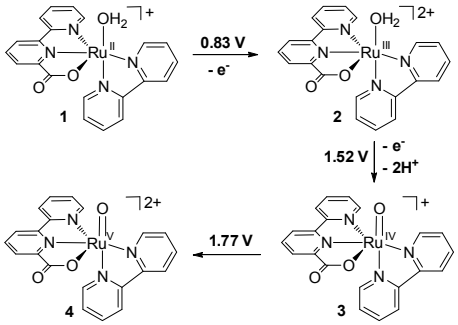

Scheme 1. Calculated redox potentials from **1** $[(bpc)(bpy)Ru^{II}OH_2]^+$ to **4** $[(bpc)(bpy)Ru^{V}=O]^{2+}$. All calculated potential values are referred to NHE.

It should be pointed out that in order to reproduce the strong hydrogen bonding interaction with the solvent precisely the geometries of the Ru-aqua complexes containing O-H bonds were optimized with additional water molecules around them by forming a reasonable hydrogen-bonding network[16], and three water molecules were added around **3** and **4** so that the reacting one at **4** is hydrogen bonded to two additional water molecules.

2) OO bond formation

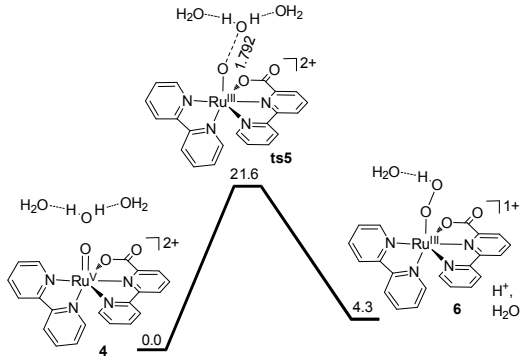

Figure 1. Profile of the calculated relative G for the coupling interaction between the oxo site of **4** and water molecule. The relative Gibbs free energies are given in kcal/mol.

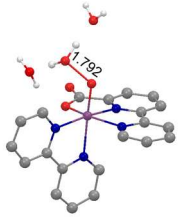

Figure 2. Optimized geometry of **ts5** in aqueous medium. Hydrogen atoms except those bonding to the O atoms are omitted for clarity (Purple for Ru, blue for N, red for O, grey for C and white for H). The bond length is given in Å.

High-valent Ru^{V}-oxo intermediates such as **4** has been proposed as active species that react with water.[17] In the reaction with water at the oxo of **4** the hydro-peroxo complex **6** $[(bpc)(bpy)Ru^{III}OOH]^+$, which contains the requisite OO bond. It is generated from a water nucleophilic attack at **4** accompanied with a proton transfer to solution. The activation energy barrier via **ts5** $[(bpc)(bpy)Ru^{III}OOH_2]^{2+}$ is calculated to be 21.6 kcal/mol (Figure 1). The simultaneous proton transfer avoids formation of a Ru-OOH_2 species, which is usually a high-energy isomer. The optimized geometry of **ts5** is shown in Figure 2. Two explicit water molecules were added during the DFT optimization, where one of the explicit water molecules plays a role of both hydrogen-bond acceptor to the aqua ligand and hydrogen-bond donor to the carboxylate O atom.

3) Formation of superoxo $7_{side\text{-}on}$ $[(bpc)(bpy)Ru^{IV}OO]^+$ and $8_{side\text{-}on}$ $[(bpc)(bpy)Ru^{V}OO]^{2+}$.

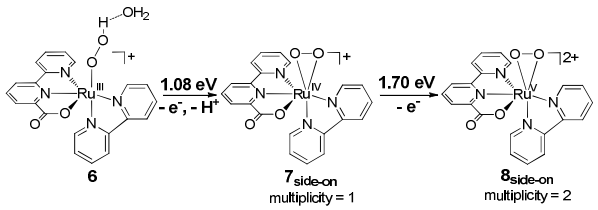

Scheme 2. Calculated redox potentials from **6** to $\mathbf{8}_{\text{side-on}}$ via $\mathbf{7}_{\text{side-on}}$.

Oxidation and deprotonation of **6** gives super-oxo $\mathbf{7}_{\text{side-on}}$ $[(bpc)(bpy)Ru^{IV}OO]^{+}$, and the redox potential is calculated to be relatively low at 1.08 V. The super-oxo $\mathbf{8}_{\text{side-on}}$ $[(bpc)(bpy)Ru^{V}OO]^{2+}$ could possibly be generated by further oxidation of $\mathbf{7}_{\text{side-on}}$ with a calculated potential of 1.70 V (Scheme 2).

There are two main configurations of the Ru super-oxo complexes, side-on configuration and end-on configuration.[18] In the side-on configuration the O_2 binds to the central Ru with an almost equal distance between the two O atoms and Ru. In the end-on configurations, one of the O atoms of O_2 is close to the Ru center while the other is not directly interacting with the metal. Both $\mathbf{7}_{\text{side-on}}$ and $\mathbf{8}_{\text{side-on}}$ are calculated to have a lower free energy in the side-on configuration and stay in their low spin states, which are singlet and doublet respectively. However, the side-on configurations of them are only slightly more stable than their end-on configurations, which will be discussed more in the following section. The possibility of formation of both $\mathbf{7}_{\text{side-on}}$ and $\mathbf{8}_{\text{side-on}}$ leads to divergent reaction pathways for oxygen release afterwards.

4) Intersystem crossing and oxygen release at $\mathbf{7}_{\text{side-on}}$.

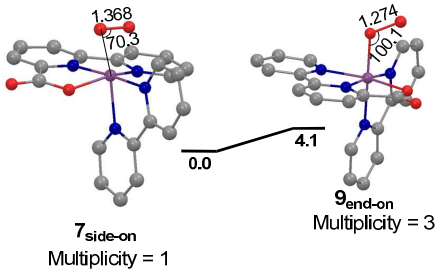

Figure 3. Gibbs free energy for the conversion from $\mathbf{7}_{\text{side-on}}$ to $\mathbf{9}_{\text{end-on}}$ $[(bpc)(bpy)Ru^{IV}OO]^{+}$. Hydrogen atoms are omitted for clarity (Purple for Ru, blue for N, red for O and grey for C). The bond length is given in Å and the bond angle is given in degree. The relative Gibbs free energies are given in kcal/mol.

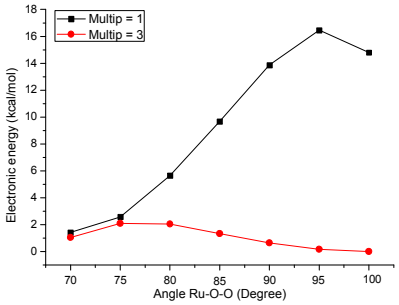

Figure 4. Scan result of intersystem crossing conversion from $\mathbf{7}_{\text{side-on}}$ to $\mathbf{9}_{\text{end-on}}$ $[(bpc)(bpy)Ru^{IV}OO]^{+}$. Plot of black points are singlet and red points are triplet. The electronic energies were obtained using Becke's three-parameter hybrid functional and the LYP correlation functional (B3LYP) together with the LACVP** core potential and basis set.

For the Ru^{IV} super-oxo complexes reported before in the literature, the crystallographic characterization confirmed a seven-coordinate structure with a side-on configuration.[19] However, since O_2 is triplet in its ground state the related super-oxo complex is proposed to stay in a high spin state to meet the spin requirement before triplet oxygen release. A spin conversion from the low spin state (singlet) $\mathbf{7}_{\text{side-on}}$ to a high spin state (triplet) $\mathbf{9}_{\text{end-on}}$ $[(bpc)(bpy)Ru^{IV}OO]^{+}$ should therefore occur before oxygen generation. We calculated that the free energy of $\mathbf{7}_{\text{side-on}}$ is lower by 4.1 kcal/mol with respect to that of $\mathbf{9}_{\text{end-on}}$, indicating that $\mathbf{7}_{\text{side-on}}$ (singlet) is the more stable state, where the distances between Ru center and two O atoms of O_2 are similar, the bond length of the dioxygen ligand is 1.368 Å and the angle Ru-O-O is 70.3°. Through an intersystemcrossing[20] it will isomerize to the complex $\mathbf{9}_{\text{end-on}}$ (triplet), which is related to the oxygen release afterwards, where the bond length of dioxygen ligand decreases to 1.274Å, and the angle Ru-O-O increased to 100.1° (Figure 3). From a relaxed coordinate scan of the Ru-O-O angle at both the low and high spin states we find that $\mathbf{7}_{\text{side-on}}$ to $\mathbf{9}_{\text{end-on}}$ (Figure 4), we find that the electronic energies of both the high spin state and the low spin state at 70° are close to identical. We therefore believe that the conversion to the high spin state $\mathbf{9}_{\text{end-on}}$ followed by barrierless conversion from the side-on complex $\mathbf{7}_{\text{side-on}}$ is facile.

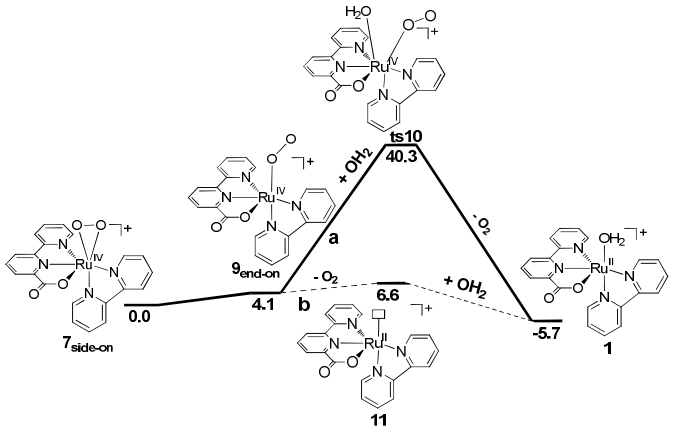

Figure 5. Oxygen generation at $\mathbf{7}_{\text{side-on}}$. a) The concerted associative pathway; b) The dissociated pathway. The relative Gibbs free energies are given in kcal/mol.

Two possible mechanistic scenarios for oxygen generation were considered starting from $\mathbf{9}_{\text{end-on}}$ (Figure 5). One is the concerted associative pathway **a**, where the evolution of O_2 occurs simultaneously with one water molecule entering. The free energy barrier via **ts10** $[(bpc)(bpy)Ru^{IV}(OH_2)O_2]^+$ is calculated at 40.3 kcal/mol. The other one is the dissociative pathway **b**, where O_2 is dissociated from $\mathbf{9}_{\text{end-on}}$ firstly, generating a five-coordinated intermediate **11** $[(bpc)(bpy)Ru^{II}]^+$, where the free energy of **11** is only 6.6 kcal/mol relative to $\mathbf{9}_{\text{side-on}}$. In order to estimate the upper limit of such reaction we performed a relaxed coordinate scan of the Ru-O distance at $\mathbf{9}_{\text{end-on}}$. The scan result of dissociation of oxygen (Figure S2), shows that the electronic energy barrier of dissociation of O_2 from $\mathbf{9}_{\text{end-on}}$ is only 7.3 kcal/mol. This scan result does not take into account the increased entropy as O_2 is dissociating and we therefore believe that 7.3 kcal/mol is the upper limit of the O_2 dissociation from $\mathbf{9}_{\text{end-on}}$. After comparing these two pathways, it is clear that the dissociative pathway is the only plausible pathway for oxygen evolution at room temperature at this oxidation state. Once the spin crossing conversion from $\mathbf{7}_{\text{side-on}}$ to $\mathbf{9}_{\text{end-on}}$ is completed, the following formation of aqua complex **1** by replacing dioxygen ligand with a water molecule is an exergonic reaction. The optimized geometry of **ts10** and intermediate **11** are shown in Figure 6.

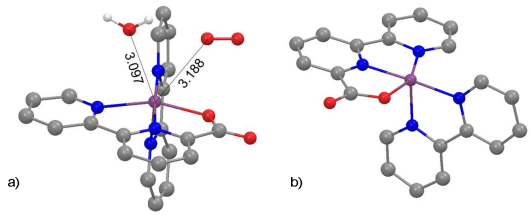

Figure 6. Optimized geometry of a) **ts10** and b) the five-coordinated intermediate **11**. Hydrogen atoms except those bonding to the O atoms are omitted for clarity (Purple for Ru, blue for N, red for O, grey for C and white for H). The bond length is given in Å.

5) Intersystem crossing and oxygen release at $\mathbf{8}_{\text{side-on}}$.

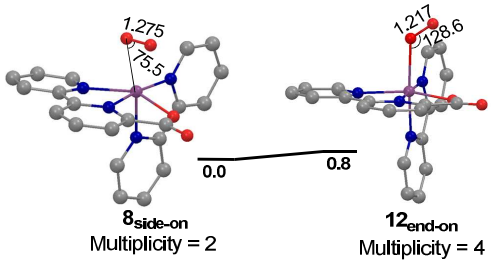

Figure 7. Intersystem crossing conversion from $\mathbf{8}_{\text{side-on}}$ to $\mathbf{12}_{\text{end-on}}$ $[(bpc)(bpy)Ru^{V}OO]^{2+}$. Hydrogen atoms are omitted for clarity (Purple for Ru, blue for N, red for O and grey for C). The bond length is given in Å and the bond angle is given in degree. The relative Gibbs free energies are given in kcal/mol.

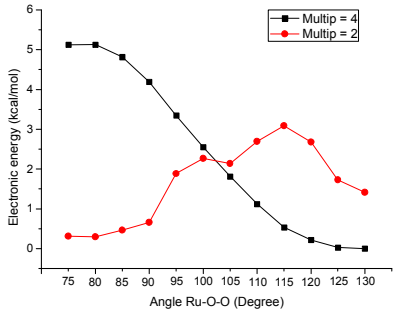

Figure 8. Scan result of intersystem crossing conversion from $\mathbf{8}_{\text{side-on}}$ to $\mathbf{12}_{\text{end-on}}$ $[(bpc)(bpy)Ru^{V}OO]^{2+}$. Plot of black points are quartet and red points are doublet. The electronic energies were obtained using Becke's three-parameter hybrid functional and the LYP correlation functional (B3LYP) together with the LACVP** core potential and basis set.

An alternative path is via further oxidation of $\mathbf{7}_{\text{side-on}}$ that gives $\mathbf{8}_{\text{side-on}}$. Conversion from the side-on $\mathbf{8}_{\text{side-on}}$ (doublet) to the end on $\mathbf{12}_{\text{end-on}}$ (quartet) is expected to occur before oxygen generation. The free energy of $\mathbf{8}_{\text{side-on}}$ is lower by merely 0.8 kcal/mol with respect to that of $\mathbf{12}_{\text{end-on}}$. In a side-on configuration the bond length of the dioxygen ligand in $\mathbf{8}_{\text{side-on}}$ is 1.275Å and the angle Ru-O-O is 75.5°. Through an intersystem crossing it will isomerize to the quartet $\mathbf{12}_{\text{end-on}}$, where the bond length of dioxygen ligand decreases to 1.217Å, and the angle Ru-O-O increased to 128.6°. The quartet $\mathbf{12}_{\text{end-on}}$ could meet the spin requirement of triplet oxygen release (Figure 7), although the doublet state in principle could dissociate to a doublet and a triplet O_2 and a doublet Ru complex. Again we calculated the intersystem crossing conversion from $\mathbf{8}_{\text{side-on}}$ to $\mathbf{12}_{\text{end-on}}$ (Figure 8), and we findthat the electronic energy of the low spin state $\mathbf{8}_{\text{side-on}}$ at 75° is lower. The calculated electronic energy of the intersystem crossing point is calculated at 2 kcal/mol above $\mathbf{8}_{\text{side-on}}$, indicating very rapid conversion to $\mathbf{12}_{\text{end-on}}$.

Similar to the reaction at the Ru^{IV} state, two possible mechanistic scenarios for oxygen generation were considered at the Ru^{V} state starting from $\mathbf{12}_{\text{end-on}}$. In the concerted associative pathway **a** the free energy barrier via **ts13** $[(bpc)(bpy)Ru^{V}(OH_2)O_2]^{2+}$is at 31.3 kcal/mol. While in the dissociative pathway **b**, the free energy of the dissociated species **14** is calculated to be -10.4 kcal/mol. It is clear that the

dissociative pathway **b** is the only plausible pathway at room temperature. With the current methodology it is difficult to calculate the activation energy of purely dissociative reactions. However, to estimate the upper limit of such reaction we performed a relaxed coordinate scan of the Ru-O distance at $\mathbf{12}_{\mathbf{end\text{-}on}}$. The scan result of dissociation of oxygen (Figure S3), shows that the electronic energy barrier of dissociation of O_2 from $\mathbf{12}_{\mathbf{end\text{-}on}}$ is 7.0 kcal/mol. As for $\mathbf{9}_{\mathbf{end\text{-}on}}$ the scan result again does not take into account the increased entropy as O_2 is dissociating and 7.0 kcal/mol is believed to be the upper limit of the O_2 dissociation from $\mathbf{12}_{\mathbf{end\text{-}on}}$. The following formation of aqua complex **2** by replacing dioxygen ligand with a water molecule occurs along an exergonic reaction path (Figure 9). The quartet $\mathbf{12}_{\mathbf{end\text{-}on}}$ produces the doublet **2** by releasing triplet O_2. The optimized geometry of **ts13** and the intermediate **14** are shown in Figure 10.

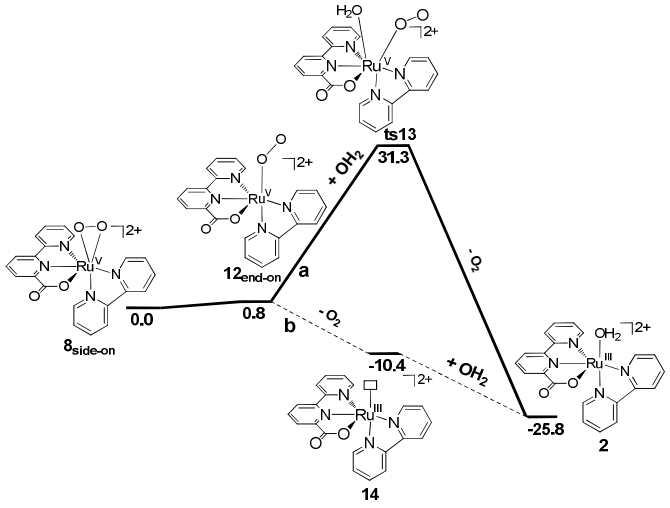

Figure 9. Oxygen generation at $\mathbf{8}_{\mathbf{side\text{-}on}}$. a) The concerted associative pathway; b) The dissociated pathway. The relative Gibbs free energies are given in kcal/mol.

After comparing the oxygen release at both $\mathbf{7}_{\mathbf{side\text{-}on}}$ and $\mathbf{8}_{\mathbf{side\text{-}on}}$, it appears that both paths are plausible and that no high activation energies were involved in the processes. The release of O_2 from $\mathbf{8}_{\mathbf{side\text{-}on}}$ was found to be more exergonic and is likely more facile.

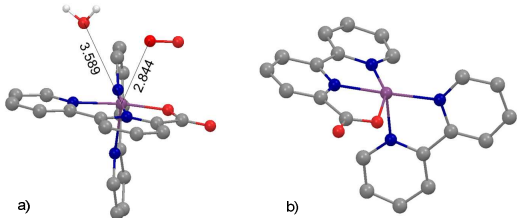

Figure 10. Optimized geometries of a) **ts13** $[(bpc)(bpy)Ru^{III}OOH_2]^{2+}$ and b) five-coordinated intermediate **14** $[(bpc)(bpy)Ru^{III}]^{2+}$. Hydrogen atoms except those bonding to the O atoms are omitted for clarity (Purple for Ru, blue for N, red for O, grey for C and white for H). The bond length is given in Å.

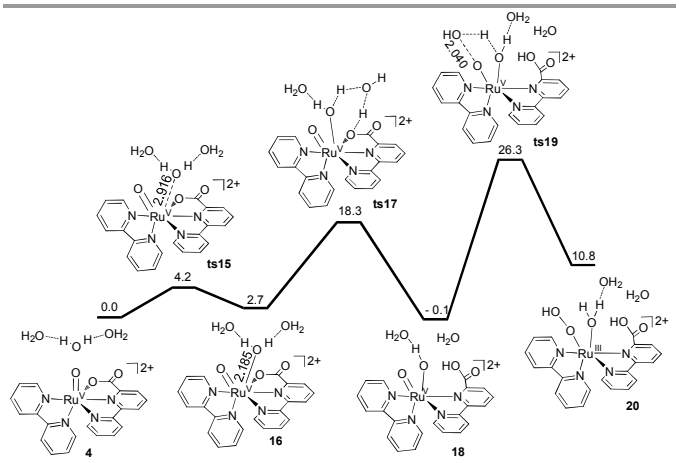

Figure 11. Profile of the calculated relative G for the reaction of water nucleophilic attack at the Ru site. The relative Gibbs free energies are given in kcal/mol and the bond length is given in Å.

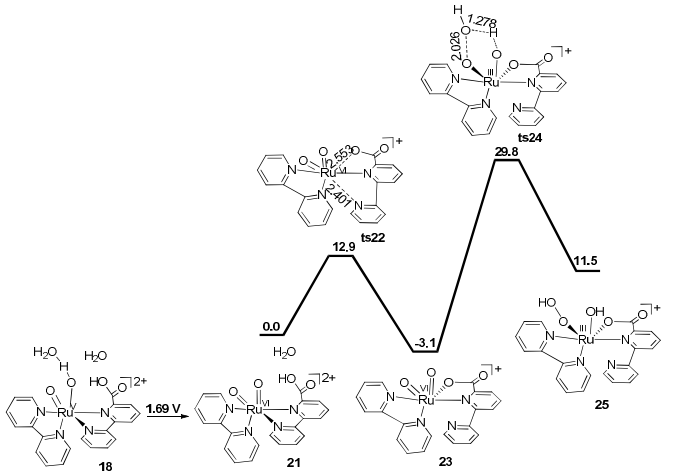

Figure 12. Profile of the calculated relative G for the reaction of OO bond formation after a further oxidation of **18**. The relative Gibbs free energies are given in kcal/mol and the bond length is given in Å.

Another possibility of the reaction of water nucleophilic attack at the metal of **4** was also examined (Figure 11). Interestingly, the reaction is very facile with a free energy barrier of only 4.2 kcal/mol via **ts15** to generate the seven-coordinate **16**. The following formation of six-coordinate **18** needs to cross over a seven-coordinate **ts17** , which is a proton transfer from the new coordinated water to the oxygen site of the carboxylate ligand via a second water molecule along with simultaneous dissociation of the carboxylate ligand, at 18.3 kcal/mol.[21] However, the following OO bond formation through water nucleophilic attack at **18** was found to be unfavorable in the catalytic cycle with an activation energy of 26.4 kcal/mol via **ts19** (OO bond formation along with concomitant transfer of a proton to the neighboring Ru-OH group). Further proton coupled electron transfer oxidation at **18** generates **21** with a calculated oxidation potential of 1.69 V (Figure 12), and the coming back of dissociated carboxylate group leads to a *cis*-bis-oxo **23** via **ts22** at 12.9 kcal/mol, water nucleophilic attack at the oxo site of **23** meets a high activation energy of 32.9

kcal/mol via **ts24**, which indicates this is quite difficult to occur at room temperature. Since *cis*-bis-oxo to *tran*-bis-oxo isomerization process was observed to take place via photoisomerization,[22] the isomerization of *cis*-bis-oxo **23** was also taken into consideration and analyzed in this paper. We found that compared to the *cis*-bis-oxo **23** the *trans* geometry of **23** has much higher free energy by 25 kcal/mol, which implies that this *trans* state is not a likely intermediate in the current reaction. The corresponding profile is available in the Supporting Information (Scheme S1). In general, the free energy barrier for water nucleophilic attack at the metal calculated is quite reasonable at room temperature, and this demonstrates another reliable proposal for the disappearance of Ru^{V}=O species observed in experiment. However, the catalytic reaction is hampered by the high activation energy requirement of OO bond formation, and this could be one possible pathway for the catalyst decay. These findings show that inclusion of a carboxylate group in the ligand could lead to new reactivity of the complex in addition to changing the properties, and that these new reaction paths could limit the lifetime of the catalyst.

Conclusions

By sequential loss of electrons and protons **1** is readily oxidized to **3**. Further oxidation gives **4**, which we find to be the most likely active species involved in the OO bond formation. Via a water nucleophilic attack, the Ru^{III} hydroperoxo **6** is generated accompanied with a proton transfer. Further oxidation of **6** gives $\mathbf{7}_{\mathbf{side\text{-}on}}$ and possibly the further oxidized $\mathbf{8}_{\mathbf{side\text{-}on}}$. Both of them have a slight preference for their low spin state, where the O_2 binds to ruthenium in a side-on configuration. Our calculated results demonstrate that oxygen release can happen at both the Ru^{IV} and Ru^{V} states. $\mathbf{7}_{\mathbf{side\text{-}on}}$ and $\mathbf{8}_{\mathbf{side\text{-}on}}$ need to transform to their high spin states with end-on configurations via an intersystem crossing, $\mathbf{9}_{\mathbf{end\text{-}on}}$ and $\mathbf{12}_{\mathbf{end\text{-}on}}$ respectively, before releasing O_2. Following a dissociative pathway O_2 is generated, and oxygen release is found to be plausible in both pathways. From the overall free energy surface of this catalytic cycle, the OO bond formation is found to be the rate-determining step in this water oxidation catalytic cycle with the catalyst **1**. Following our prior studies on the reaction of **4** with water we also investigated water oxidation pathways initiated by reaction of water at the metal site instead of at the oxo site. While the initial reaction of water at the metal center has low barriers the consequent OO bond formation step at the Ru^{V} oxo hydroxo complex **18** is blocked by high activation energy barriers. **18** can potentially also be further oxidized to the Ru^{VI} bisoxo complex **23**, but also here the reaction with water is associated with high activation energies. We therefore believe that the reactions at the metal are more likely related to degradation pathways leading to inactive catalyst. Blocking of these paths by modification of the catalyst structure could therefore lead to more robust catalysts.

Computational studies

All Density Functional Theory (DFT) calculations were carried out with Jaguar 7.6 program package by Schrödinger LLC. For geometry optimizations, solvation energy, and frequency calculations, Becke's three-parameter hybrid functional and the LYP correlation functional (B3LYP)[23] was used with the LACVP** core potential and basis set, while single point energy corrections were performed with the M06[24] functional using the LACV3P**++ basis set which, as suggested by Martin,[25] was augmented with two f-polarization functions on Ru. Frequency calculations were performed on the optimized geometries to verify that the geometries correspond to minima or first-order saddle points (transition states) on the potential energy surface (PES). The Gibbs free energies are calculated at standard state of 1 atm (g) and 1M(aq) and the G of each species is defined as the following equation $G = E(M06/LACV3P^{**}{+}{+}\ 2f\ on\ Ru) + G_{solv} + ZPE + H_{298} - TS_{298}$ + 1.9 kcal/mol (the 1.9 kcal/mol is a concentration correction to the free energy of solvation which by default is calculated at 1M(g) to 1M(aq) in Jaguar). Based on the gas-phase-optimized structures, the effect of solvent was evaluated by single-point calculations using the Poisson-Boltzmann reactive field implemented in Jaguar 7.6 (PBF)[26] in water. For the scan of intersystem crossing conversion, the electronic energies were obtained using Becke's three-parameter hybrid functional and the LYP correlation functional (B3LYP) together with the LACVP** core potential and basis set. For the water molecule we used free energy of vaporisation of -2.05 kcal/mol, which is the free energy of transferring H_2O(g) at 1 atm and H_2O (liq) at 55.5 M at 298.15 K. For the proton the experimental number[27] for the free energy of solvation of -264 kcal mol^{-1} was used (for the free energy of 1M proton in water the value of -270.3 kcal mol^{-1} was used). Our choice of functional was based on a systematic study where we compared calculated reduction potentials and p*K*a values to experimental data together. These results are described in the supplementary material of our previous paper.[21]

Acknowledgements

This research has been funded by Vetenskapsrådet and EU-Erasmus Mundus. Computational resources have been provided by the National Supercomputer Centre in Linköping, Sweden.

Notes and references

Division of Theoretical Chemistry & Biology, School of Biotechnology, KTH Royal Institute of Technology, 106 91 Stockholm, Sweden. E-mail: mahlquist@theochem.kth.se

Electronic Supplementary Information (ESI) available: [details of any supplementary information available should be included here]. See DOI: 10.1039/b000000x/

1 a) D. Gust, T. A. Moore and A. L. Moore, *Acc. Chem. Res.*, 2009, **42**, 1890-1898; b) L. Sun, L. Hammarström, B. Åkermark and S. Styring, *Chem. Soc. Rev.*, 2001, **30**, 36-49; c) M. Yagi, A. Syouji, S. Yamada, M. Komi, H. Yamazaki and S. Tajima, *Photochem. Photobiol. Sci.*, 2009, **8**, 139-147; d) R. Lomoth, A. Magnuson, M. Sjodin, P. Huang, S. Styring and L. Hammarström, *Photosynth. Res.,* 2006, **87**, 25-40.

2 a) J. Limberg, V. A. Szalai and G. W. Brudvig, *J. Chem. Soc., Dalton, Trans.*, 1999, 1353-1361; b) C. Sens, I. Romero, M. Rodriguez, A. Llobet, T. Parella and J. Benet-Buchholz, *J. Am. Chem. Soc*., 2004**, 126**, 7798-7799; c) I. Romero, M. Rodriguez, C. Sens, J. Mola, M. R. Kollipara, L. Francas, E. Mas-Marza, L Escriche and A. Llobet, *Inorg. Chem*., 2008, **47**, 1824-1834; d) Y. V. Geletii, Z. Huang, Y. Hou, D. G. Musaev, T. Lian and C. L. Hill, *J. Am. Chem. Soc*., 2009, **131**, 7522-7523; f) C. W. Chronister, R. A. Binstead, J. Ni and T. J. Meyer, *Inorg. Chem*., 1997, **36**, 3814-3815; e) E. L. Lebeau, S. A. Adeyemi and T. J. Meyer, *Inorg. Chem*., 1998, **37**, 6476-6484; f) J. J. Concepcion, J. W. Jurss, J. L. Templeton and J. M. Thomas, *J. Am. Chem. Soc*., 2008**, 130**, 16462-16463;

3 a) N. Kaveevivitchai, R. Zong, H-W. Tseng, R. Chitta and R. P. Thummel, *Inorg. Chem*., 2012, **51**, 2930-2939; b) Z. Deng, H-W. Tseng, R. Zong, D. Wang and R. Thummel, *Inorg. Chem*., 2008, **47**, 1835-1848; c) H-W. Tseng, R. Zong, J. T. Muckerman and R. Thummel, *Inorg. Chem*., 2008, **47**, 11763-11773.

4 a) J. D. Blakemore, N. D. Schley, D. Balcells, J. F. Hull, G. W. Olack, C. D. Incarvito, O. Eisenstein, G. W. Brudvig and R. H. Crabtree, *J. Am. Chem. Soc*., 2010, **132**, 16017-16029; b) N. D. McDaniel, F. J. Coughlin, L. L. Tinker and D. Bernhard, *J. Am. Chem. Soc*., 2008**, 130**, 210-217.

5 a) D. K. Dogutan, Jr, R. McGuire and D. G. Nocera, *J. Am. Chem. Soc*., 2011**, 133**, 9178-9180; b) S. M. Barnett, K. I. Goldberg and J. M. Mayer, *Nature. Chem*., 2012, **4**, 498-502; c) S. Enthaler, K. Junge and M. Beller, *Angew. Chem. Int. Ed*., 2008, **47**, 3317-3321; d) J. L. Fillol, Z. Codolà, I. Garcia-Bosch, L. Gomez, J. J. Pla and M. Costas, *Nat. Chem.*, 2011, **3**, 807-813.

6 S. W. Gersten, G. J. Samuels and T. J. Meyer, *J. Am. Chem. Soc*., 1982**, 104**, 4029-4030.

7 a) Y. Xu, T. Åkermark, V. Gyollai, D. Zou, L. Eriksson, L. Duan, R. Zhang, B. Åkermark and L. Sun, *Inorg. Chem*., 2008, **48**, 2717-2719; b) L. Duan, Y. Xu, P. Zhang, M. Wang and L. Sun, *Inorg. Chem*., 2010, **49**, 209-215; c) L. Duan, Y. Xu, L. Tong and L. Sun, *ChemSusChem.*, 2011, **4**, 238-244; d) L. Tong, Y. Wang, L. Duan, Y. Xu, X. Cheng, A. Fischer, M. S. G. Ahlquist and L. Sun, *Inorg. Chem*., 2012, **51**, 3388-3398. e) L. Duan, C. M. Araujo, M. S. G. Ahlquist, L. Sun *Proc. Natl. Acad. Sci. U.S.A.* 2012, 109, 15584-15588. f) R. Staehle, L. Tong, L. Wang, L. Duan, A. Fischer, M. S. G. Ahlquist, L. Sun, S. Rau *Inorg. Chem.* 2014, **53**, 1307-1319.

8 a) J. Barber and B. Andersson, *Nature*, 1994, **370**, 31-34; b) G. Renger, *Physiol. Plant.*, 1997, **100**, 828-841; c) J. Barber, *Inorg. Chem*., 2008, **47**, 1700-1710; d) J. Yano and V. K. Yachandra, *Inorg. Chem*., 2008, **47**, 1711-1726.

9 J. J. Concepcion, M-K. Tsai, J. T. Muckerman and T. J. Meyer, *J. Am. Chem. Soc*., 2010**, 132**, 1545-1557.

10 a) X. Yang and M-H. Baik, *J. Am. Chem. Soc*., 2008, **130**, 16231-16240; b) A. Sartorel, M. Carraro, F. Scorrano, R. De Zorzi, S. Geremia, N. D. McDaniel, S. Bernhard and M. Bonchio, *J. Am. Chem. Soc*., 2008**, 130**, 5006-5007.

11 F. Bozoglian, S. Romain, M. Z. Ertem, T. K. Todorova, C. Sens, J. Mola, M. Rodriguez, I. Romero, J. Benet-Buchholz, X. Fontrodona, C. J. Cramer, L. Gagliardi and A. Llobet, *J. Am. Chem. Soc*., 2009**, 131**, 15176-15187.

12 a) L. Duan, A. Fischer, Y. Xu and L. Sun, *J. Am. Chem. Soc*., 2009**, 131**, 10397-10399; b) J. Nyhlén, L. Duan, B. Åkermark, L. Sun and T. Privalov. *Angew. Chem., Int. Ed.*, 2010, **49**, 1773-1777.

13 I. López, M. Z. Ertem, S. Maji, J. Benet-Buchholz, A. Keidel, U. Kuhlmann, P. Hildebrandt, C. J. Cramer, V. S. Batista and A. Llobet, *Angew. Chem. Int. Ed*., 2014, **53**, 205-209.

14 L. Tong, A. Ken Inge, L. Duan, L. Wang, X. Zou and L. Sun, *Inorg. Chem*., 2013, **52**, 2505-2518.

15 a) M. Sjödin, S. Styring, B. Åkermark, L. Sun and L. Hammarström, *J. Am. Chem. Soc*., 2000**, 122**, 3932-3936; b) J. D. Soper, S. V. Kryatov, E. V. Rybak-Akimova and D. G. Nocera, *J. Am. Chem. Soc*., 2007, **129**, 5069-5075; c) S. Hammes-Schiffer, *Acc. Chem. Res.* 2009, **42**, 1881-1889.

16 a) Y. Umena, K. Kawakami, J. R. Shen and N. Kamiya, *Nature*, 2011, **473**, 55-60; b) B. C. Polander and B. A. Barry, *Proc. Natl. Acad. Sci*. U.S.A., 2012, **109**, 1-6.

17 a) X. Liu and F. Y. Wang, *Coord. Chem. Res*., 2012, **256**, 1115-1136; b) J. S. Vrettos, J. Limburg and G. W. Brudvig, *Biochimica ET Biophysica ACTA-Bioenergetics*, 2001, **1503**, 229-245; c) J. J. Concepcion, J. W. Jurss, M. K. Brennaman, P. G. Hoertz. A. O. T. Patrocinio, N. Y. M. Iha, J. L. Templeton and J. M. Thomas, *Acc. Chem. Res*., 2009, **42**, 1954-1965; d) F. Liu, J. J. Concepcion, J. W. Jurss, T. Cardolaccia, J. L. Templeton and J. M. Thomas, *Inorg. Chem*., 2008, **47**, 1727-1752.

18 a) L. Pauling, *Nature*, 1964, **203**, 182-183; b) J. S. Griffith, *Proc. R. Soc. Lond. A*, 1956, **235**, 23-26.

19 a) J. Shen, E. D. Stevens and S. P. Nolan, *Organometallics*, 1998, **17**, 3875-3882; b) I. de los Rios, M. J. Tenorio, J. Padilla, M. C. Puerta and P. Valerga, *J. Chem. Soc., Dalton Trans*., 1996, **3**, 377-381; c) E. Lindner, M. Haustein, R. Fawzi, M. Steimann and P. Wegner, *Organometallics*, 1994, **13**, 5021-5029.

20 a) T. Chachiyo and J. H. J. Rodriguez, *J. Chem. Phys.*, 2005, **123**, 094711-094719; b) M. Bearpark, M. Robb and H. Schlegel, *Chem. Phys. Lett*., 1994, **223**, 269-274; c) R. Poli and J. Harvey, *Chem. Soc. Rev.,* 2003, **32**, 1-8; d) M. Robb, M. Garavelli, M. Olivucci and F. Bernardi, *Rev. Comput. Chem*., 2000, **15**, 87-146.

21 Y. Wang and M. S. G. Ahlquist, *Phys. Chem. Chem. Phys.,* 2014, **16**, 11182-11185.

22 a) J. C. Dobson and T. J. Meyer, *Inorg. Chem*, 1988, **27**, 3283-3291; b) X. Sala, M. Z. Ertem, L. Vigara, T. K. Todorova, W. Chen, R. C. Rocha, F. Aquilante, C. J. Cramer, L. Gagliardi and A. Llobet, *Angew. Chem. Int. Ed*., 2010, **49**, 7745-7747.

23 a) A. D. Becke, *J. Chem. Phys.,* 1993, **98**, 5648-5652; b) C. Lee, W. Yang and R. G. Parr, *Phys. Rev. B,* 1988, **37**, 785-789.

24 Y. Zhao and D. G. Truhlar, *Theor. Chem. Acc.,* 2006, **120**, 215-241.

25 J. M. L. Martin and A. Sundermann, *J. Chem. Phys.*, 2001, **114**, 3408-3420.

26 B. Marten, K. Kim, C. Cortis, R. A. Friesner, R. B. Murphy, M. N. Ringnalda, D. Sitkoff and B. Honig, *J. Phys. Chem.*, 1996, **100**, 11775-11788.

27 M. D. Tissandier, K. A. Cowen, W. Y. Feng, E. Gundlach, M. H. Cohen, A. D. Earhart and J. V. Coe, *J. Chem. Phys. A,* 1998, **102**, 7787-7794.